Available online at www.sciencedirect.com
ScienceDirect
Journal of Colloid and Interface Science 303 (2006) 243–249
JOURNAL OF Colloid and Interface Science
www.elsevier.com/locate/jcis

EPS biofouling in membrane filtration: An analytic modeling study

Albert S. Kim [a,*], Huaiqun Chen [b], Rong Yuan [c]

[a] *Civil and Environmental Engineering, University of Hawaii at Manoa, 2540 Dole Street, Honolulu, HI 96822, USA*
[b] *Hawaii Pacific Engineers Inc., 1132 Bishop Street, Honolulu, HI 96813, USA*
[c] *Department of Mathematics, Qingdao University, Qingdao, Shandong 266071, PR China*

Received 18 April 2006; accepted 19 July 2006

Available online 29 July 2006

Abstract

Biofouling is theoretically investigated by modeling solute transport within a biofilm, defined in this study as a swarm of solid biocolloids surrounded by liquid-like exopolymeric substances (EPS). A mathematical approach is employed to map the biofilm to an equivalent, simple spherical cell using a self-consistent method. It is found that the physical presence of EPS and their reaction with solute ions reduce the mass transfer coefficient, which significantly contributes to permeate flux decline in reverse osmosis and nanofiltration membrane processes.

Keywords: Diffusive tortuosity factor; Biofouling; Biofilm; Biocolloids; Extracellular polymeric substances (EPS); Back-diffusion

1. Introduction

Biofouling in pressure-driven membrane filtration has received close attention in past decades because the fouling causes severe performance loss, modifies membrane surface properties, and requires costly periodic cleaning or membrane replacement. Of concern are biological species that excrete a protective mass of polysaccharides known as EPS—extracellular polysaccharides or exopolymeric substances [1]. EPS that cover bacteria cells serve to entrap nutrient species and, more important, to impede transport of biocides that would efficiently kill bacteria in the planktonic state [2].

Conventional colloidal (solid) cakes formed on reverse osmosis (RO) and nanofiltration (NF) membrane surfaces do not provide a noticeable increase in hydraulic cake resistance but significantly promote concentration polarization (CP) of solutes by hindering their back-diffusion. Therefore, a second-step flux decline occurs due to enhanced osmotic pressure [3,4], and this phenomenon is well explained by employing a diffusive tortuosity factor of porous medium [5] (i.e., cake layer with different structures [6]). High solute concentration of the feed water of RO/NF processes suppresses electrostatic repulsion between particles, leaving the Van der Waals attraction as the dominant interparticle interaction. If the colloidal concentration of the feed stream is relatively high, colloidal aggregation may occur in the bulk phase, and the formed cake layer will have higher porosity and hence lower hydraulic resistance due to the sparse structure of aggregates. Therefore, flux decline stemming from the colloidal aggregation is less in comparison to that of the conventional cake layer composed of individual particles. While solid cakes provide only physical obstruction with solute back-diffusion, a soft cake (i.e., biofilm) composed of EPS-covered biocolloids (such as bacteria) causes physical as well as chemical hindrance on solute diffusion. Colonies of EPS-covered bacteria not only generate flow channeling followed by increased brine concentration but also enhance the osmotic pressure by entrapping solutes within EPS layers and so hinder their diffusion away from the membrane surface. Therefore, biofouling in RO/NF processes must be investigated in both biological and physical aspects: rapid proliferation of EPS-producing bacteria on the membrane surfaces (i.e., increasing biofilm thickness) and solute penetration into the biofilm (i.e., partitioning of solutes in the bulk and EPS phases).

A plethora of researchers have investigated diffusion phenomena within biofilms using various experimental techniques

* Corresponding author. Fax: +1 (808) 956 5014.
E-mail address: AlbertSK@hawaii.edu (A.S. Kim).
URL: http://pam.eng.hawaii.edu.

0021-9797/$ – see front matter
doi:10.1016/j.jcis.2006.07.067

such as microelectrodes [7,8], fiberoptic microsensors [9], nuclear magnetic resonance spectroscopy [10,11], infrared spectroscopy combined with Raman microscopy [12], and confocal laser scanning microscopy [13–15]. Although some of the experimental results were well explained using the hindered diffusion concept, effects of physical and chemical hindrances are somewhat ambiguously combined into a single quantity, i.e., diffusive tortuosity factor. The experimental techniques listed above cannot measure separately the effects of the physical presence of EPS (generated on biocolloid surfaces) and their partitioning of salt ions rejected by the membrane and retained within the deposit layer. Moreover, it is not feasible to implement such experimental techniques into the dynamic operations of RO/NF processes to monitor the degree of biofouling. In this light, a conceptual model that can reflect the presence and reaction of EPS into filtration performance is of great necessity to specifically understand the effects of hindered solute back-diffusion on flux decline in RO/NF processes due to EPS.

2. Theory

For a complete description of mass transport through the biofilm layer, a full convection–diffusion–reaction (CDR) equation should be solved using the material properties of biofilms and solutes. The three (separate) transport mechanisms (of CDR) are, in general, incorporated into the governing equation using the linear superposition principle. In other words, the overall mass transport is described as the linear sum of the three CDR contributions. In this light, this study focuses only on diffusive solute flux through the biofilm layer composed of EPS-covered bacteria and investigates mean (phenomenological) effects on permeate flux decline.

Experimental visualization shows that EPS-producing bacteria usually have helical or rod-like shapes [16]. When the helical-shaped bacteria are sufficiently long, a cylindrical model can be developed, assuming that the thickness is negligible relative to the length. (Related mathematical approaches for permeability of cylinder-packed porous media are fully described elsewhere [17].) On the other hand, rod-shaped bacteria are relatively short, having oval shapes with small eccentricities close to zero. For mathematical simplicity, the current model employs spherical-shaped bacteria, mapping the short rod-shaped ones to volume-equivalent spheres.

Fig. 1 shows a three-dimensional image of a swarm of monodispersed composite spheres. Each composite sphere consists of a solid biocolloid of radius a (shown as a dark sphere), covered with an EPS layer of thickness δ (shown as a semi-transparent sphere). The EPS layer, produced by biocolloids, is a gel-like, liquid-state polymeric material into which solutes can diffuse but water cannot freely penetrate.

Fig. 2 depicts the swarm of composite spheres in a diffusive cell model. Any composite sphere embedded in the swarm sees all the other spheres as an exterior porous body in a self-consistent manner. The porous body is then regarded as a uniform, isotropic continuum medium with void spaces into which solutes can diffuse.

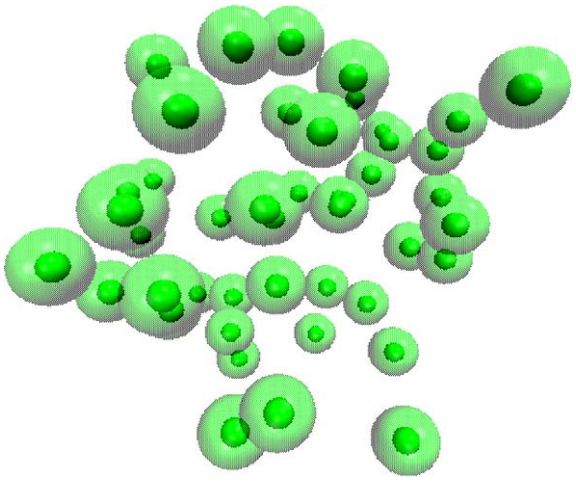

Fig. 1. Schematic of biocolloids covered with EPS.

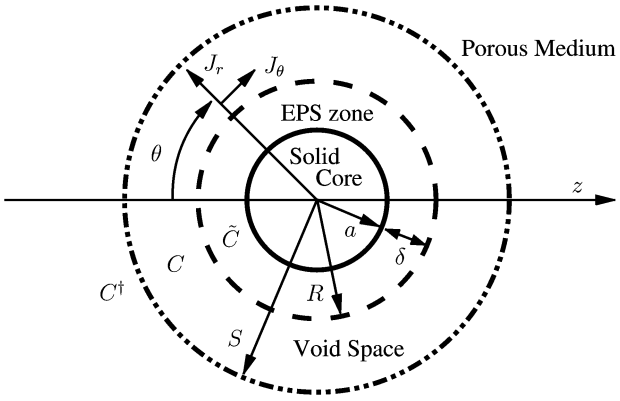

Fig. 2. Descriptive diagram of the diffusive cell model.

2.1. Governing equations

In the void space ($R < r < S$), solute diffusion is represented by Fick's law, given as

$$\vec{J} = -D_0 \nabla C \tag{1}$$

and time-invariance of the solute concentration simplifies the continuity equation to

$$\nabla \cdot \vec{J} = 0. \tag{2}$$

Substitution of Eq. (1) into Eq. (2) with a constant diffusivity D_0 yields

$$\nabla^2 C = 0. \tag{3}$$

By using azimuthal symmetry, one can write general solutions for concentrations in regions of porous medium, void space, and EPS as

$$C^\dagger(S \leqslant r < \infty, \theta) = \sum_{n=0}^{\infty} \left[A_n r^n + B_n r^{-(n+1)}\right] P_n(\cos\theta), \tag{4}$$

$$C(R \leqslant r \leqslant S, \theta) = \sum_{n=0}^{\infty} \left[E_n r^n + F_n r^{-(n+1)}\right] P_n(\cos\theta), \tag{5}$$

and

$$\tilde{C}(a < r \leqslant R, \theta) = \sum_{n=0}^{\infty} \left[G_n r^n + H_n r^{-(n+1)} \right] P_n(\cos\theta), \tag{6}$$

respectively, where $P_n(\theta)$ is the Legendre polynomial such as

$$\begin{aligned} &P_0(\cos\theta) = 1, \\ &P_1(\cos\theta) = \cos\theta, \\ &P_2(\cos\theta) = \frac{1}{2}\left(3\cos^2\theta - 1\right), \\ &\ldots. \end{aligned} \tag{7}$$

Then, radial and tangential components of the diffusive flux in each region are as follows:

$$\begin{aligned} J_r^{\dagger} &= -D^{\dagger}\frac{\partial C^{\dagger}}{\partial r} \\ &= -D^{\dagger}\sum_{n=0}^{\infty}\left[n A_n r^{n-1} - (n+1) B_n r^{-(n+2)} \right] P_n(\cos\theta), \end{aligned} \tag{8}$$

$$\begin{aligned} J_{\theta}^{\dagger} &= -\frac{D^{\dagger}}{r}\frac{\partial C^{\dagger}}{\partial \theta} \\ &= D^{\dagger}\sum_{n=0}^{\infty}\left[A_n r^{n-1} + B_n r^{-(n+2)} \right] P_n'(\cos\theta)\sin\theta, \end{aligned} \tag{9}$$

$$\begin{aligned} J_r &= -D_0\frac{\partial C}{\partial r} \\ &= -D_0\sum_{n=0}^{\infty}\left[n E_n r^{n-1} - (n+1) F_n r^{-(n+2)} \right] P_n(\cos\theta), \end{aligned} \tag{10}$$

$$\begin{aligned} J_{\theta} &= -\frac{D_0}{r}\frac{\partial C}{\partial \theta} \\ &= D_0\sum_{n=0}^{\infty}\left[E_n r^{n-1} + F_n r^{-(n+2)} \right] P_n'(\cos\theta)\sin\theta, \end{aligned} \tag{11}$$

$$\begin{aligned} \tilde{J}_r &= -\tilde{D}\frac{\partial \tilde{C}}{\partial r} \\ &= -\tilde{D}\sum_{n=0}^{\infty}\left[n G_n r^{n-1} - (n+1) H_n r^{-(n+2)} \right] P_n(\cos\theta), \end{aligned} \tag{12}$$

$$\begin{aligned} \tilde{J}_{\theta} &= -\frac{\tilde{D}}{r}\frac{\partial \tilde{C}}{\partial \theta} \\ &= \tilde{D}\sum_{n=0}^{\infty}\left[G_n r^{n-1} + H_n r^{-(n+2)} \right] P_n'(\cos\theta)\sin\theta, \end{aligned} \tag{13}$$

where

$$P_n'(\cos\theta) = \left.\frac{\mathrm{d}P_n(x)}{\mathrm{d}x}\right|_{x=\cos\theta}. \tag{14}$$

The EPS layer, often negatively charged, is where biodegradation may occur when the feed contains certain organic matters. In this study, however, we employ a simple model by considering only inorganic solutes and assume that the chemical and biological properties of the EPS layer are effectively reflected in the solute diffusivity, $\tilde{D}$.

2.2. Boundary conditions

Boundary conditions employed in this study are

$$\begin{aligned} \vec{J}^{\dagger}(S,\theta) &= Q\hat{z} = -Q\cos\theta\hat{r} + Q\sin\theta\hat{\theta} \\ &= J_r^{\dagger}(S,\theta)\hat{r} + J_{\theta}^{\dagger}(S,\theta)\hat{\theta}, \end{aligned} \tag{15}$$

$$C(S,\theta) = C^{\dagger}(S,\theta), \tag{16}$$

$$J_r(S,\theta) = J_r^{\dagger}(S,\theta), \tag{17}$$

$$\tilde{C}(R,\theta) = \sigma C(R,\theta), \tag{18}$$

$$\tilde{J}_r(R,\theta) = J_r(R,\theta), \tag{19}$$

$$\tilde{J}_r(a,\theta) = -U, \tag{20}$$

where Q is a constant flux throughout the entire porous medium, and $\hat{r}$ and $\hat{\theta}$ are the unit vectors in the radial and tangential directions, respectively. Equations (16) and (17) indicate continuities of the concentration and radial flux at $r = S$, i.e., the interface between the void space and porous medium. Equation (18) is used to introduce partitioning of solutes between the EPS and bulk phases, characterized by the partitioning coefficient σ at $r = R$, where the radial fluxes are continuous from Eq. (19). Equation (20) describes the flux of solutes from the EPS zone due to bacteria, which maintain (specific) solute concentrations within the cell by controlling the direction of the uptake flux. Bacteria use solutes as food if U is positive, but solutes are released with a negative value of U. This uptake flux, however, is assumed to be negligible in comparison with actual solute flux within the RO/NF membrane channel. Moreover, in a dormant state U disappears. Therefore, the uptake flux U is set to zero, and the proliferation of bacteria contributes to an increase in biofilm thickness. The porosity of the entire porous medium is then calculated as

$$\epsilon = 1 - \phi_R, \tag{21}$$

where

$$\phi_R = \left(\frac{R}{S}\right)^3, \tag{22}$$

which indicates the fraction of biofilm volume from which water is excluded.

2.3. Solutions

The orthogonality of the Legendre polynomial indicates that unknown coefficients (A_n to H_n) are related to each other for a given polynomial order n. Because the ambient solute flux of Eq. (15) only contains $P_1(\cos\theta) = \cos\theta$ and $\frac{\mathrm{d}P_1(\cos\theta)}{\mathrm{d}\theta} = -\sin\theta$ terms, all the coefficients of the second and higher orders should be zero in all three regions, that is

$$A_n = B_n = E_n = F_n = G_n = H_n = 0 \quad \text{for } n \geqslant 2. \tag{23}$$

In addition, A_0 is a reference concentration of an arbitrary constant so that setting $A_0 = 0$ does not change any results because the current study focuses on the concentration gradient. Therefore, all the coefficients of the zeroth order are also zero:

$$A_0 = B_0 = E_0 = F_0 = G_0 = H_0 = 0. \tag{24}$$

Meaningful solutions that satisfy Eqs. (15)–(20) then have the following forms:

$$A_1 = \frac{Q}{D^\dagger}, \tag{25}$$

$$B_1 = 0, \tag{26}$$

$$E_1 = \left(\frac{Q}{3D_0}\right)\left(\frac{2}{d_{\mathrm{PM}}} + 1\right), \tag{27}$$

$$F_1 = \left(\frac{Q}{3D_0}\right)\left(\frac{1}{d_{\mathrm{PM}}} - 1\right)S^3, \tag{28}$$

$$G_1 = \sigma\frac{E_1 + F_1 R^{-3}}{1 + \frac{1}{2}\phi_a}, \tag{29}$$

$$H_1 = \frac{1}{2}a^3 G_1, \tag{30}$$

where

$$d_{\mathrm{PM}} = \frac{D^\dagger}{D_0} \tag{31}$$

and

$$\phi_a = \left(\frac{a}{R}\right)^3. \tag{32}$$

Here, ϕ_a indicates the fraction of the solid core within the composite sphere. The explicit functional form of d_{PM}, the ratio of the effective diffusivity in the porous media to the bulk diffusivity in free space, is obtained by equating two different expressions for H_1 (or G_1) from Eqs. (18) and (19):

$$d_{\mathrm{PM}} = \frac{(1 + \frac{1}{2}\phi_a)(1 - \phi_R) + \frac{1}{2}\sigma d_{\mathrm{EPS}}(1 - \phi_a)(1 + 2\phi_R)}{(1 + \frac{1}{2}\phi_a)(1 + \frac{1}{2}\phi_R) + \frac{1}{2}\sigma d_{\mathrm{EPS}}(1 - \phi_a)(1 - \phi_R)}, \tag{33}$$

where

$$d_{\mathrm{EPS}} = \frac{\tilde{D}}{D_0}, \tag{34}$$

which is the diffusivity ratio in the EPS layer and void space. Therefore, the effective solute diffusivity within the biofilm, $D^\dagger$ ($=d_{\mathrm{PM}}D_0$), can be analytically represented as a function of D_0, ϕ_a, ϕ_R, σ, and d_{EPS}.

2.4. Confirmation of solution: Absence of the EPS layer

The dimensionless effective diffusivity within a porous medium composed of monodispersed spheres of radius a, in the absence of EPS, can be obtained by taking the limits of $d_{\mathrm{EPS}} = 0$ and/or $R \to a$:

$$d_{\mathrm{PM}} = \frac{1 - \phi}{1 + \frac{1}{2}\phi}, \tag{35}$$

where

$$\phi = \left(\frac{a}{S}\right)^3. \tag{36}$$

Here, $\sigma d_{\mathrm{EPS}} = 0$ indicates zero solute concentration within the EPS layer or the forbidden diffusive flux into the EPS zone that becomes a part of the solid core, and $R \to a$ implies the physical absence of the EPS layer with a zero EPS-thickness.

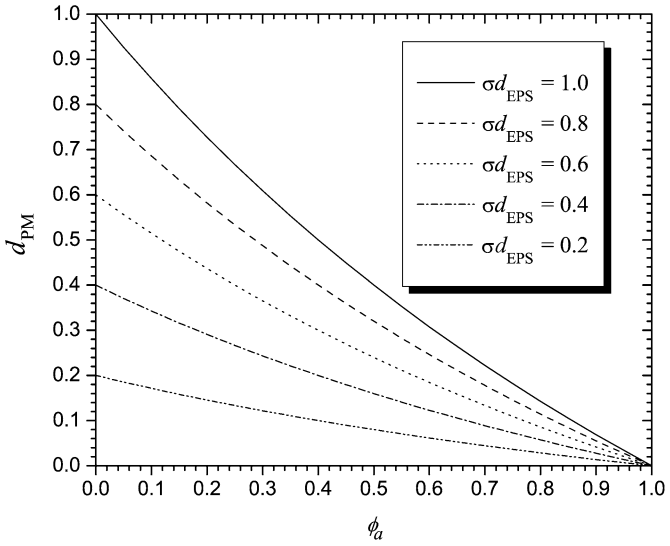

Fig. 3. Dimensionless effective diffusivity in the porous medium with $\phi_R = 1.0$.

Anther way to represent the absence of the EPS layer is to change the EPS to the solvent, equivalently, $d_{\mathrm{EPS}} = 1$, with the continuity of concentration at the EPS–bulk interface (i.e., $\sigma = 1$). Within this limit, Eq. (33) again becomes

$$d_{\mathrm{PM}} = \frac{1 - \phi}{1 + \frac{1}{2}\phi}. \tag{37}$$

Equations (35) and (37), having the same mathematical form, are identical to the analytic expression from Maxwell's [18] and Neale and Nader's works [19], which is plotted as the top solid line in Fig. 3. The denominators of Eqs. (35) and (37), termed the *diffusive tortuosity factor*, were extensively studied with several model structures of sphere-packed porous medium [6].

3. Results and discussion

3.1. Effects of EPS on solute diffusivity

The dimensionless effective diffusivity d_{PM} of Eq. (33) indicates roles of partitioning and diffusion of solutes within the EPS layer, characterized by σ and d_{EPS}, respectively. While both are insignificant, i.e., $\sigma d_{\mathrm{EPS}} \ll 1$, d_{PM} becomes similar to the conventional hindered diffusion case [18,19]. For the opposite case, higher diffusivity within the EPS layer effectively enhances overall diffusion through the biofilm, which is physically equivalent to accommodating more effective void spaces within the biofilm. The effects of partitioning and diffusion are discussed below.

Fig. 3 shows the effective diffusivity with different values of σd_{EPS} when the void spaces are completely filled with EPS, i.e., $\phi_R = 1$. Water permeation through the porous medium becomes practically negligible, and the diffusive transport is mainly through the EPS region in which solutes diffuse with $\tilde{D}$. The solid line for $\sigma d_{\mathrm{EPS}} = 1.0$ indicates that EPS act like water, and the corresponding d_{PM} is identical to the previous work [18,19]. As σd_{EPS} decreases from 1.0 to zero, the effective diffusivity has a similar decreasing trend. Note that values of d_{PM}

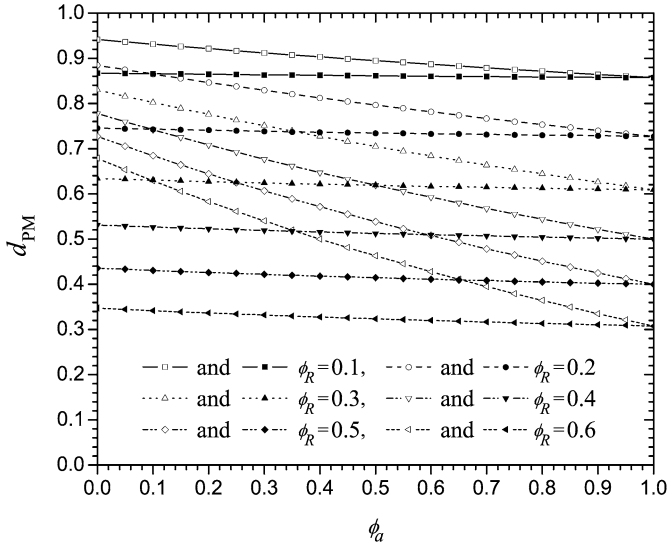

Fig. 4. Dimensionless effective diffusivity in the porous medium with $\sigma d_{EPS} = 0.5$ (hollow symbols) and 0.05 (solid symbols).

with $\phi_a = 0$ in Fig. 3 are equal to corresponding values of σd_{EPS}. When $\phi_R = 1$, ϕ_a becomes equivalent to the fraction of solid region from which solutes are excluded. As the solute diffusivity within the EPS layer decreases (but does not reach zero), solutes stay longer within the EPS layers, and in extreme cases they are (almost entirely) trapped within the layer.

Fig. 4 shows variations of the effective diffusivity with respect to ϕ_a, given σd_{EPS} and ϕ_R. Knowing that the maximum random packing ratio is about 0.6 for monodispersed solid spheres [20–22], we select two σd_{EPS} values and span ϕ_R from 0.1 to 0.6 with an interval of 0.1. Within EPS layers, $\sigma d_{EPS} = 0.5$ and 0.05 imply half and negligible solute diffusivity in comparison to the bulk diffusivity D_0 if $\sigma = 1$. Decreasing trends of d_{PM} with respect to ϕ_a remain apparent for $\sigma d_{EPS} = 0.5$ but obscure for $\sigma d_{EPS} = 0.05$: these effects stem from the second terms in the numerator and the denominator of Eq. (33). As ϕ_a reaches 1.0, d_{PM} values with $\sigma d_{EPS} = 0.5$ and 0.05 converge to the same value with a given ϕ_R, which indicates the absence of the EPS layer. Note that d_{PM} values with $\phi_a = 1$ in Fig. 4 are equal to those of Fig. 3 with $\sigma d_{EPS} = 1$ after ϕ_a of Fig. 3 is replaced by ϕ_R of Fig. 4. As ϕ_R increases, d_{PM} decreases, which implies that as void spaces decrease, solutes should take more convoluted routes within less void spaces while some of them stay within EPS layers.

When EPS layers are absent, the numerator $1-\phi$ of Eq. (35) becomes equivalent to the fraction of void spaces (i.e., porosity) in which solutes can diffuse. The denominator of Eq. (35) is termed the diffusive tortuosity factor, which quantifies the tortuousness of porous media as a function of solid volume fraction [6]. In the same light, it can be interpreted that the numerator of Eq. (33) corresponds to effective fractional space in which solutes can undergo diffusive transport, and the denominator represents effective tortuousness of the biofilm in the presence of EPS. However, individual analyses of the numerator and denominator of Eq. (33) do not provide independent physical meanings so that only the ratio should be treated as the dimensionless effective diffusivity of solutes within the biofilm.

3.2. Implication on biofouling

Structural heterogeneity of the biofilm often generates a unique flow field, which reduces physical stresses on bacteria in the interstitial flow field. A certain portion of water and solute mass is transported through the void network of the biofilm due to the transmembrane pressure. The concepts of structural heterogeneity and void network are, however, highly dependent on the interaction of bacteria with the flow field under the high pressure of RO/NF processes. In this light, to provide a simple phenomenological understanding of EPS effects on the permeate flux decline, we follow Hoek et al.'s work [3] by employing film theory as a basic flux analysis method:

$$v_w = k^* \ln\left(\frac{C_m - C_p}{C_b - C_p}\right) = k^* \ln\left(\frac{\Delta C_m}{\Delta C_b}\right), \tag{38}$$

where v_w is the permeate velocity, and C_m, C_b, and C_p are solute concentrations (molarity) on the membrane surface, in the bulk phase, and in the permeate stream, respectively. Here, k^* is the mass transfer coefficient defined as [3]

$$\frac{1}{k^*} = \frac{\delta_c}{D^\dagger} + \frac{\delta_p}{D_0} = \frac{1}{D_0}\left(\frac{\delta_c}{d_{PM}} + \delta_p\right), \tag{39}$$

where δ_c and δ_p are thicknesses of the biofilm layer and solute CP (above the biofilm), respectively, in this study. The filtration equation for RO/NF, based on the solution–diffusion model [23], is represented as

$$v_w = \frac{\Delta P - \Delta\pi}{\mu(R_m + R_c)}, \tag{40}$$

where ΔP is the transmembrane pressure, R_m is the intrinsic membrane resistance, and R_c is the hydraulic resistance of the biofilm. Note that $1-\phi_R$ should be used as volume fraction of solvent flow to theoretically estimate R_c using the Carman–Kozeny equation [24] or Happel's cell model [25]. Here, $\Delta\pi$ is the osmotic pressure difference between the membrane surface and permeate stream, represented by Van't Hoff's equation:

$$\Delta\pi = R_g T \Delta C_m, \tag{41}$$

where R_g is the universal gas constant and T is the absolute temperature. Using Eqs. (38) and (41), Eq. (40) can be rewritten as

$$R_g T \Delta C_b e^J + \mu R_T k^* J = \Delta P, \tag{42}$$

where R_T $(=R_m + R_c)$ is the total resistance and J $(=v_w/k^*)$ is the dimensionless permeate flux. Equation (38) indicates that if the CP modulus, C_m/C_b, does not exceed e^1 (=2.718), then J is less than 1.0. In this case, e^J can be expanded, using the Taylor series, as $e^J \simeq 1 + J + \frac{1}{2!}J^2 + \cdots$, so J can be approximately represented as

$$J = (1 + \hat{R}_T)\left(-1 + \sqrt{1 + \frac{2(\Delta\hat{P} - 1)}{(1 + \hat{R}_T)^2}}\right), \tag{43}$$

where

$$\hat{R}_T = \frac{\mu R_T k^*}{\Delta\pi_b}, \tag{44}$$

$$\Delta\hat{P} = \frac{\Delta P}{\Delta\pi_b}, \tag{45}$$

$$\Delta\pi_b = R_g T \Delta C_b. \tag{46}$$

When the pressure is high enough to easily overcome the bulk osmotic pressure $\Delta\pi_b$ as well as $(\mu R_T k^*)^2/\Delta\pi_b$, Eq. (43) is further simplified to

$$v_w = k^* \sqrt{\frac{2\Delta P}{\Delta\pi_b}}, \tag{47}$$

implying that the permeate flux is proportional to the square root of the applied pressure. If the feed concentration is very low, providing a negligible osmotic pressure, Eq. (47) seems to diverge. This is because the transmembrane pressure does not exceed $(\mu R_T k^*)^2/\Delta\pi_b$. Taking a limit of zero, feed concentration in Eq. (43) returns to Eq. (40) with vanishing osmotic pressure. On the other hand, if the bulk osmotic pressure is less than but close to the applied pressure, Eq. (43) can be approximated as

$$v_w = k^* \frac{\Delta P - \Delta\pi_b}{\mu R_T k^* + \Delta\pi_b}, \tag{48}$$

indicating a linear relationship between the permeate flux and applied pressure. In conjunction with Eq. (39), Eqs. (47) and (48) point out that the permeate flux does decline with respect to decreasing k^*, e.g., decreasing the effective solute diffusivity $D^\dagger$ $(=D_0 d_{\mathrm{PM}})$ within the biofilm.

For a lower solute diffusivity $\tilde{D}$ within the EPS layer, solutes can stay longer in a steady state while slowly diffusing within the layer and forming a certain concentration profile. This scenario effectively reduces the overall solute diffusivity $D^\dagger$ within the entire biofilm. Mathematically, reduced mass transfer coefficient k^* with decreasing $D^\dagger$ explains the corresponding flux decline in Eqs. (47) and (48). A physical interpretation is as follows. The partitioning of concentration at the EPS–void interface (Eq. (18)) implies that higher solute concentration within the biofilm due to the lower $D^\dagger$ enhances the concentration within void spaces of the biofilm and also the wall concentration C_m. We would like to call it EPS-enhanced concentration polarization, which can further increase the osmotic pressure. A relationship between k^* and $\Delta\pi$ can be obtained by equating Eqs. (38) and (40) with Eq. (41):

$$k^* = \frac{\Delta P - \Delta\pi}{\mu R_T \ln(\Delta\pi/\Delta\pi_b)}, \tag{49}$$

which elucidates that solvent mass transfer from the bulk phase to permeate stream is hindered by enhanced osmotic pressure. In the same light, the permeate flux can decline with increasing ϕ_a and/or ϕ_R (or thicker δ) or decreasing d_{EPS}, which all effectively hinder solute back-diffusion away from the vicinity of the membrane surface towards the top of the CP layer.

Particulate fouling in RO/NF membrane processes can be categorized into two cases: colloidal fouling and biofouling. Colloidal particles in the solid cake layer physically hinder the solute back-diffusion by playing roles as geometrical obstacles. Osmotic pressure enhancement by the solid cake layer has therefore only a physical aspect along the membrane channel. On the other hand, a few bacteria alive in the membrane channel due to imperfect disinfection and/or pretreatment can generate colonies composed of a tremendous number of multiplicated bacteria. Excreted materials from the bacteria form liquid-like EPS, and hence the biofilm has physical softness (i.e., deformability) and chemical reactiveness through the effective diffusivity. The soft EPS layer provides additional hydraulic resistance by decreasing void spaces for permeate flow as well as solute diffusion. The reactiveness of EPS hinders the solute back-diffusion by providing local nesting spaces with diffusing solutes. Partitioning of solutes in the void and EPS regions enhances the wall concentration and osmotic pressure in a sequential way. Therefore, it is sufficient to say that biofouling is more deleterious than colloidal fouling from both the physical and chemical point of view. Property changes of membrane materials due to attachment and growth of bacteria can cause further (remarkable) performance loss in RO/NF membrane filtration.

4. Conclusions

The spherical, diffusive cell model (as an extension of Neale and Nader's work [19]) is developed to investigate the hindered solute diffusion within the biofilm formed on the membrane surface. The diffusive tortuosity of the biofilm is analytically calculated as a function of solute diffusivity within EPS layers, thickness of EPS layer, solute partitioning coefficient, and porosity of the biofilm. The presence of EPS on surfaces of biocolloids reduces void fraction for water permeation, and the reactivity of EPS holds solutes within the EPS layer so that their back-diffusion (from the membrane surface to the bulk phase across the biofilm) is effectively hindered. A small solute diffusivity within the EPS layer (less than that in the bulk phase) produces higher concentration within the EPS layer as well as at the boundary of EPS–voids. The continuity of solute concentration at the boundary induces higher solute concentration within the entire biofilm. Therefore, hindered back-diffusion generates EPS-enhanced concentration polarization and, accordingly, enhanced osmotic pressure on the membrane surface. The diffusive tortuosity of the biofilm influences the permeate flux via the mass transfer coefficient of film theory.

Acknowledgments

This research was made possible by a grant from the US National Science Foundation Faculty Early Career (CAREER) Development Program (CTS04-49431) and the US Geological Survey, through the Water Resources Research Center, University of Hawaii at Manoa, Honolulu. (This is contributed Paper CP-2006-09 of the Water Resource Research Center.)

References

[1] H.C. Flemming, G. Schaule, Desalination 70 (1–3) (1988) 95–119.

[2] S.B. Sadr Ghayeni, P.J. Beatson, R.P. Schneider, A.G. Fane, J. Membr. Sci. 138 (1) (1998) 29–42.
[3] E.M.V. Hoek, A.S. Kim, M. Elimelech, Environ. Eng. Sci. 19 (6) (2002) 357–372.
[4] E.M.V. Hoek, M. Elimelech, Environ. Sci. Technol. 37 (24) (2003) 5581–5588.
[5] B.P. Boudreau, Geochim. Cosmochim. Acta 60 (16) (1996) 3139–3142.
[6] A.S. Kim, H. Chen, J. Membr. Sci. 279 (2006) 129–139.
[7] H. Beyenal, A. Tanyolac, Z. Lewandowski, Water Sci. Technol. 38 (8–9) (1998) 171–178.
[8] K. Rasmussen, Z. Lewandowski, Biotechnol. Bioeng. 59 (3) (1998) 302–309.
[9] H. Beyenal, Z. Lewandowski, C. Yakymyshyn, B. Lemley, J. Wehri, Appl. Opt. 39 (19) (2000) 3408–3412.
[10] E.E. Beuling, D.v. Dusschoten, P. Lens, J.C.v.d. Heuvel, H.V. As, S.P.P. Ottengraf, Biotechnol. Bioeng. 60 (3) (1998) 283–291.
[11] M. Vogt, H.C. Flemming, W.S. Veeman, J. Biotechnol. 77 (1) (2000) 137–146.
[12] P.A. Suci, G.G. Geesey, B.J. Tyler, J. Microbiol. Methods 46 (3) (2001) 193–208.
[13] D. deBeer, P. Stoodley, Z. Lewandowski, Biotechnol. Bioeng. 53 (2) (1997) 151–158.
[14] J.R. Lawrence, G.M. Wolfaardt, D.R. Korber, Appl. Environ. Microbiol. 60 (4) (1994) 1166–1173.
[15] M. Kuehn, M. Mehl, M. Hausner, H.-J. Bungartz, S. Wuertz, Water Sci. Technol. 43 (6) (2001) 143–151.
[16] American Water Works Association Research Foundation, Water Treatment Membrane Processes, McGraw–Hill, New York, 1996.
[17] J. Happel, H. Brenner, Low Reynolds Number Hydrodynamics, Prentice–Hall, Englewood Cliffs, NJ, 1965.
[18] J.C. Maxwell, Treatise on Electricity and Magnetism, Dover, New York, 1881.
[19] G. Neale, W.K. Nader, AIChE J. 19 (1) (1973) 112–119.
[20] G.T. Nolan, P.E. Kavanagh, Powder Technol. 72 (1992) 149–155.
[21] G.Y. Onoda, E.G. Liniger, Phys. Rev. Lett. 64 (22) (1990) 2727–2730.
[22] W. Soppe, Powder Technol. 62 (1990) 189–196.
[23] H.K. Lonsdale, U. Merten, R.L. Riley, J. Appl. Polym. Sci. 9 (1965) 1341–1362.
[24] P.C. Carman, Trans. Inst. Chem. Eng. 15 (1937) 150–156.
[25] J. Happel, AIChE J. 4 (1958) 197–201.